Slab flattening, magmatism, and surface uplift in the Cordillera Occidental (northern Peru)

Audrey Margirier, Xavier Robert, Laurence Audin, Cécile Gautheron, Matthias Bernet, Sarah Hall, Thibaud Simon-Labric

Publisher: GSA
Journal: GEOL: Geology
DOI:10.1130/G37061.1

Slab flattening, magmatism and surface uplift in the Cordillera Occidental (northern Peru)

Audrey Margirier[1], Xavier Robert[1,2], Laurence Audin[1,2], Cécile Gautheron[3], Matthias Bernet[1], Sarah Hall[4], and Thibaud Simon-Labric[5]

[1]Université de Grenoble-Alpes, ISTerre, F-38041 Grenoble, France

[2]Institut de recherche pour le développement (IRD), ISTerre, F-38041 Grenoble, France

[3]Université Paris Sud, UMR GEOPS-CNRS 8148, 91405 Orsay, France

[4]College of Atlantic, 105 Eden Street, Bar Harbor, Maine 04609, USA

[5]IDYST, University of Lausanne, CH-1015 Lausanne, Switzerland

ABSTRACT

The impact of subduction processes on surface uplift and relief building in the Andes is not well understood. In northern Peru we have access to a modern flat subduction zone (3–15°S) where both the geometry and timing of the flattening of the slab are well constrained. Some of the highest Andean peaks, the Cordillera Blanca (6768 m) and the Cordillera Negra (5187 m), are located just above the Peruvian flat-slab. This is a perfect target to explore the impact of slab flattening and associated magmatism on the Andean topography and uplift. We present new apatite (U-Th)/He and fission-track data from three vertical profiles in the Cordillera Blanca and the Cordillera Negra. Time-temperature inverse modeling of the thermochronological data suggest that regional exhumation in the Cordillera Occidental started at ~15 Ma, synchronous with the onset of subduction of the Nazca Ridge and eastward movement of regional magmatism. We propose that ridge subduction at 15 Ma and onset of slab flattening drove regional surface

uplift, with an important contribution of magmatism to relief building in the Cordillera Occidental.

INTRODUCTION

The Andes are often presented as the classic example of relief building along a non-collisional convergent plate boundary, but many subduction zone processes, specifically related to surface uplift, are still not fully understood. Along the western Andean margin topography and slab dip vary significantly, resulting in a clear segmentation along strike, with two modern flat-slab segments in northern Peru (3–15°S; Fig. 1) and central Chile (28–32°S) (Barazangi and Isacks, 1976). These flat-slab subduction zones influence the occurrence and location of magmatic activity along the Andean range with the magmatic arc migrating away from the trench and even ceasing to exist during slab flattening. Slab flattening also increases coupling at the plate interface, resulting in an increase and eastward displacement of shortening in the overriding plate and consequent surface uplift in both the Andean fore-arc and back-arc (e.g., Ramos and Folguera, 2009). However, the impact of slab flattening on surface uplift in the western part of the Andes (Cordillera Occidental) remains unclear.

The geometry and timing of slab flattening in northern Peru are constrained by the subduction of two buoyant features, the Nazca Ridge and the Inca Plateau (e.g., Gutscher et al., 1999; Rosenbaum et al., 2005). In this region the Cordillera Blanca (CB), a Miocene batholith exhumed along a ~150 km long crustal-scale normal fault trending parallel to the range, forms the highest Peruvian peaks (Fig. 1; e.g., McNulty and Farber, 2002). In the context of flat subduction, which is expected to produce shortening, the presence of this major normal fault is surprising. Two models have been proposed to

Publisher: GSA
Journal: GEOL: Geology
DOI:10.1130/G37061.1

explain the Cordillera Blanca Normal Fault (CBNF). Dalmayrac and Molnar (1981) suggested that extension was induced by gravitational collapse of a thickened crust, whereas McNulty and Farber (2002) suggested extension due to the arrival of the Nazca Ridge beneath this region, which temporarily increased the coupling with the overriding plate. Understanding the exhumation of the CB and extension along the CBNF in this compressive regime is important for understanding the impact of ridges and flat subduction on the Andean relief development.

The aim of this paper is to evaluate the relationship between changes in geodynamics and relief evolution in the Cordillera Occidental in northern Peru. We infer relief evolution from apatite (U-Th)/He (AHe) and fission-track (AFT) data of the CB and the Cordillera Negra (CN). We compare time-temperature inverse modeling (QTQt; Gallagher, 2012) with the timing of the arrival of the Nazca Ridge at the subduction zone, periods of magmatic activity, and periods of uplift.

GEOLOGIC AND GEODYNAMIC CONTEXT

Reconstructions of the timing and location of the initial Nazca Ridge subduction and its subsequent southeastward migration constrain the timing of slab flattening (e.g., McNulty and Farber, 2002; Rosenbaum et al., 2005). These reconstructions are based on symmetric seafloor-spreading in a hotspot reference frame, and rely on the calculation of the Nazca Plate motion with respect to South America, which may contain considerable errors. Rosenbaum et al. (2005) presented a regionally refined plate circuit that suggests ridge subduction beginning at 15 Ma at 10°S and the arrival of the Inca Plateau at the trench at 5°S at 13 Ma (Fig. 1).

Publisher: GSA
Journal: GEOL: Geology
DOI:10.1130/G37061.1

The CB is a 14–5 Ma granitic pluton (zircon U-Pb; Mukasa, 1984; Giovanni, 2007) intruded into Jurassic sediments. The high summits of the CB build the footwall of the CBNF, which has produced > 4500 m of vertical offset since 5 Ma (Bonnot, 1984; Giovanni, 2007). The Callejón de Huaylas, a 150 km long range-parallel intra-mountain basin, separates the CB and the CN. The 8–3 Ma Yungay ignimbrites, in the northern part of the basin (Farrar and Noble, 1976; Cobbing et al., 1981; Wise and Noble, 2003), and 5.4 ± 0.1 Ma ignimbrites at the base of the stratigraphy of this basin, constrain the timing of basin formation in relation to CBNF activity (Giovanni et al., 2010). The CB batholith and synchronous volcanic deposits indicate the last activity before the cessation of magmatism (Petford and Atherton, 1992) associated with slab flattening.

The Cretaceous and Paleogene plutons (73–48 Ma; Beckinsale et al., 1985) intruded into Jurassic sediments of the CN forms a plateau with summits > 5000 m and 1–2 km-deep valleys incised into its western flank. Some Neogene volcano-sedimentary deposits cap the CN (54–15 Ma Calipuy Formation; Cobbing et al., 1981). Few studies have addressed volcanism in the CN (Farrar and Noble, 1976; Myers, 1976; Noble et al., 1990), and no thermochronologic data are currently available. In the CB, few AFT and AHe data are available, mostly from glacial valleys along longitudinal profiles (Montario, 2001; Giovanni, 2007; Hodson, 2012). Thermochronological data outside of our CB and CN study areas are limited (Wipf, 2006, Michalak, 2013, Eude et al., 2015), preventing any regional thermal modeling. Due to the absence of thermochronologic data in the CN, earlier exhumation models focused on the CBNF.

METHODS

Publisher: GSA
Journal: GEOL: Geology
DOI:10.1130/G37061.1

AFT and AHe thermochronology record the temperature evolution of the crust from 120 to 40°C (e.g., Gallagher et al., 1998; Gautheron et al., 2009), which can be related to local exhumation or thermal events. Although thermochronological data do not allow direct quantification of surface uplift, with complementary information exhumation can be interpreted to be the result of surface uplift and enhanced erosion. We determine the thermal history for a vertical profile using the QTQt software, which inverts AFT annealing and AHe diffusion parameters with the Markov Chain Monte Carlo method (Gallagher, 2012; details on sample processing, analysis and modeling are provided in the GSA data repository[1]). We use the multikinetic annealing model of Ketcham et al. (2007) to model the AFT ages and track-length dispersion and the recoil damage model of Gautheron et al. (2009) to model AHe ages.

NEW THERMOCHRONOLOGICAL DATA

We sampled three profiles with elevations spanning 0.9–1.9 km, one in the CB batholith (>10 km from the CBNF to avoid a tectonic exhumation signal) and two in the CN, providing 33 AFT ages, track-length measurements and single-grain AHe ages for 23 samples (Fig. 1). The AFT ages in the CB range from 1.5 ± 0.3–7.7 ± 1.1 Ma and AHe ages range from 1.9 ± 0.2–13.7 ± 1.4 Ma (Fig. 1). The AHe ages are scattered and older than AFT ages, raising the question of their reliability. Indeed, ^{4}He implantation from an external U-Th source can generate 50% of excess He and cause age dispersion (Gautheron et al., 2012). In the CN AFT ages range from 21.1 ± 1.3–33.2 ± 1.9 Ma and AHe ages range from 1.9 ± 0.2–32.6 ± 3.3 Ma.

TIME TEMPERATURE INVERSION

Publisher: GSA
Journal: GEOL: Geology
DOI:10.1130/G37061.1

Thermal inversion of the CB age-elevation profile indicates rapid cooling at ~200°C/m.y. between 4.5 and 4 Ma following batholith emplacement at high temperatures (Fig. 2). This rapid cooling is bracketed by the batholith emplacement ages (14–5 Ma; Mukasa, 1984; Giovanni, 2007) and AFT ages. At ~4 Ma the cooling rate decreased to 25°C/m.y.

Inverse modeling of the northern CN suggests an initial cooling stage between 30 and 23 Ma, followed by a progressive reheating between 23 and 15 Ma (Fig. 2). Between 15 Ma and today the rocks cooled at 7°C/m.y. The southern CN model indicates an initial cooling episode between 30 and 18 Ma, and then a 18-15 Ma heating event. From 15 Ma to today the rocks recorded a cooling phase with a rate around 7°C/m.y. (Fig. 2). For both CN profiles, the obtained Temperature-time (Tt) paths indicate slow cooling during the Oligocene followed by reheating during the Early Miocene and finally monotonic cooling since ~15 Ma (Fig. 2).

DISCUSSION

Middle Miocene Exhumation of the Northern Peruvian Andes

Both CN profiles indicate reheating of the crust over several million years before 15 Ma and subsequent cooling. This progressive reheating likely corresponds to regional heating during emplacement of the volcanic Calipuy Formation (54–15 Ma; Cobbing et al., 1981). The presence of the Calipuy magmatic arc possibly increased the geothermal gradient in the Cordillera Occidental.

The cause of the onset of exhumation recorded by the cooling phase in the CN between 15 and 0 Ma is not straightforward. Pollen analyses constrained a maximum possible elevation of 2 km in the Peruvian Andes before the Middle Miocene (Hoorn et

Publisher: GSA
Journal: GEOL: Geology
DOI:10.1130/G37061.1

al., 2010). At that time, the CN formed the drainage divide (Fig. 3A; Wise and Noble, 2003). McLaughlin (1924) suggested that the CN Jurassic sediments, deposited near sea level, were uplifted and eroded to a low relief surface (Puna surface) until ~15 Ma, during the Quechua 1 deformation event. This surface is presently located at ~4400 m a.s.l.. Late Miocene volcanic rocks (7.4 Ma, Wipf, 2006) fill a paleovalley (now reincised) along the Rio Fortaleza, which has its headwaters in the CN. This morphology records a change in base level indicating that some uplift and incision occurred between 15 and 7 Ma (Farrar and Noble, 1976, Myers, 1976). Giovanni et al. (2010) showed from $\delta^{18}O$ analyses of paleolake deposits that high elevations in the Callejon de Huaylas basin (Fig. 1) were attained by latest Miocene times. Therefore, the cooling recorded at 15 Ma in the CN is likely related to erosion triggered by regional surface uplift. This scenario is consistent with previous studies bracketing the uplift of the Western Andes of northern Peru between the Early and Late Miocene (e.g., Farrar and Noble, 1976, Myers, 1976; Giovanni et al., 2010; Hoorn et al., 2010).

Ridge Subduction, Slab Flattening and Surface Uplift

The initiation of exhumation at ~15 Ma in the CN correlates with subduction of the Nazca Ridge (Fig. 3B; Rosenbaum et al., 2005). Exhumation in the CN continued after initial ridge subduction and its southward migration until today (Figs. 3C, 3D). The timing (15 Ma) and location (10°S) of the initial Nazca Ridge subduction proposed by Rosenbaum et al. (2005) is consistent with the Middle Miocene continental shelf uplift at this latitude (von Huene and Suess, 1988), with the propagation of the orogenic front toward the east at ~8 Ma (Mégard, 1987), and with the shift of magmatic sources toward the east from the Calipuy Formation (54–15 Ma; Cobbing et al., 1981) to the CB magmas

(CB batholith, Fortaleza and Yungay ignimbrites, 14–3 Ma; Mukasa, 1984; Wise and Noble, 2003; Wipf, 2006; Giovanni, 2007; Giovanni et al., 2010). Eakin et al. (2014) suggested that slab flattening has an influence on the evolution of the overriding plate and proposed ~1000 m positive dynamic topography in the Cordillera Occidental after slab flattening. As no important compressive phase has been documented during the Middle Miocene in the Cordillera Occidental in northern Peru (Mégard, 1987), we suggest that regional uplift resulted from positive dynamic topography above the flat-slab.

Magmatism and Exhumation in the Cordillera Blanca

The CB thermal history indicates rapid cooling (200°C/m.y.) of the batholith followed by slower cooling (25°C/m.y) beginning ~4 Ma. The rapid cooling likely corresponds to the post magmatic cooling of the CB batholith; coeval exhumation is not excluded. The slower cooling likely corresponds to exhumation. This cooling rate suggests higher exhumation rates in the CB than in the CN. Following McNulty et al. (1998) and Petford and Atherton (1992), we propose that strike-slip faulting facilitated the earlier stage of CB exhumation (Fig. 3C). Our data combined with previously published thermochronologic data (U-Pb and Ar-Ar; Giovanni, 2007) indicate that the CB emplacement and onset of exhumation are coeval, suggesting that the crustal emplacement of low-density magma participated in the exhumation of the CB (Petford and Atherton, 1992). The presence of polished granitic clasts in Pliocene sediments indicates glacial erosion of the CB (Bonnot, 1984), placing the CB at elevations at least in excess of ~3500 m at this time. Finally, we suggest that magmatism and glacial erosion (Fig. 3D) continued to drive the local CB uplift and exhumation in a context of regional surface uplift following slab flattening.

Publisher: GSA
Journal: GEOL: Geology
DOI:10.1130/G37061.1

The CB exhumation cannot be explained with models involving increased coupling at the plate interface and shortening in the upper plate. Such models are not compatible with extension related to the CBNF. The initiation of the CBNF (~5.4 Ma; Giovanni et al., 2010) is ~10 Myr after the subduction of the Nazca Ridge (15 Ma; Rosenbaum et al., 2005), demonstrating that the subduction of the ridge does not control extension on the CBNF and CB exhumation, as suggested by McNulty and Farber (2002). Collapse models (e.g., Dalmayrac and Molnar, 1981) are in contradiction with the 15–0 Ma exhumation of the CN. We suggest that the fault is accommodating the differential exhumation of the two cordilleras.

SUMMARY

Thermochronological data and temperature-time history modeling, suggest exhumation since 15 Ma in the CN. We interpret this exhumation phase as the result of elevated erosion rates in response to regional surface uplift. This scenario is in agreement with other studies bracketing the timing of uplift of the Cordillera Occidental between the Early and Late Miocene (e.g., Hoorn et al., 2010), but contradicts models of extensional or gravitational collapse of thickened crust (e.g., Dalmayrac and Molnar, 1981). We propose that surface uplift in the Cordillera Occidental was driven by the Nazca Ridge subduction, slab flattening, and associated magmatism (i.e., CB magmas). By constraining the timing of heating and cooling of upper crustal rocks from the late Oligocene to the present, this study provides new evidence linking flat subduction to the topographic evolution of the northern Peruvian Andes.

ACKNOWLEDGMENTS

This work was supported by a grant from Labex OSUG@2020 (Investissements d'avenir – ANR10 LABX56), ECOS-NORD/COLCIENCIAS/ICETEX and SMINGUE. We thank the SERNAMP for allowing sampling in the CB, and F. Coeur, F. Senebier, E. Hardwick, M. Balvay, R. Pinna-Jamme, K. Hodson and M. Michalak for sample preparation. We thank C. Lithgow and two anonymous reviewers for their constructive reviews.

REFERENCES CITED

Barazangi, M., and Isacks, B.L., 1976, Spatial distribution of earthquakes and subduction of the Nazca plate beneath South America: Geology, v. 4, p. 686–692, doi:10.1130/0091-7613(1976)4<686:SDOEAS>2.0.CO;2.

Beckinsale, R.D., Sanchez-Fernandez, A.W., Brook, M., Cobbing, E.J., Taylor, W.P., and Moore, N.D., 1985. Rb–Sr whole-rock isochron and K–Ar age determinations for the Coastal Batholith of Peru, *in* Pitcher, W.S., and Atherton, M.P., eds., Magmatism at a Plate Edge: The Peruvian Andes: Glasgow, Blackie, p. 177–202.

Bonnot, D., 1984, Néotectonique et tectonique active de la Cordillère Blanche et du Callejon de Huaylas (Andes nord-péruviennes) [Thesis (unpublished)]: Centre d'Orsay, Université de Paris-Sud, p. 1–202.

Cobbing, J., Pitcher, W., Baldock, J., Taylor, W., McCourt, W., and Snelling, N.J., 1981, Estudio geológico de la Cordillera Occidental del norte del Perú: Instituto Geologico Minero y Metalurgico, Serie D. Estudios Especiales, v. 10, no. D., p. 1-252

Dalmayrac, B., and Molnar, P., 1981, Parallel thrust and normal faulting in Peru and constraints on the state of stress: Earth and Planetary Science Letters, v. 55, p. 473–481, doi:10.1016/0012-821X(81)90174-6.

226 Eakin, C.M., Lithgow-Bertelloni, C., and Dávila, F.M., 2014, Influence of Peruvian flat-
227 subduction dynamics on the evolution of western Amazonia: Earth and Planetary
228 Science Letters, v. 404, p. 250–260, doi:10.1016/j.epsl.2014.07.027.
229 Eude, A., Roddaz, M., Brichau, S., Brusset, S., Calderon, Y., Baby, P., and Soula, J.C.,
230 2015, Controls on timing of exhumation and deformation in the northern Peruvian
231 eastern Andean wedge as inferred from low-temperature thermochronology and
232 balanced cross section: Tectonics, v. 34, p. 715–730, doi:10.1002/2014TC003641.
233 Farrar, E., and Noble, D.C., 1976, Timing of late Tertiary deformation in the Andes of
234 Peru: Geological Society of America Bulletin, v. 87, p. 1247–1250,
235 doi:10.1130/0016-7606(1976)87<1247:TOLTDI>2.0.CO;2.
236 Gallagher, K., 2012, Transdimensional inverse thermal history modeling for quantitative
237 thermochronology: Journal of Geophysical Research, v. 117, B02408,
238 doi:10.1029/2011JB008825.
239 Gallagher, K., Brown, R., and Johnson, C., 1998, Fission track analysis and its
240 applications to geological problems: Annual Review of Earth and Planetary
241 Sciences, v. 26, no. 1, p. 519–572, doi:10.1146/annurev.earth.26.1.519.
242 Gautheron, C., Tassan-Got, L., Ketcham, R.A., and Dobson, K.J., 2012, Accounting for
243 long alpha-particle stopping distances in (U-Th-Sm)/He geochronology: 3D
244 modeling of diffusion, zoning, implantation, and abrasion: Geochimica et
245 Cosmochimica Acta, v. 96, p. 44–56, doi:10.1016/j.gca.2012.08.016.
246 Gautheron, C., Tassan-Got, L., Barbarand, J., and Pagel, M., 2009, Effect of alpha-
247 damage annealing on apatite (U–Th)/He thermochronology: Chemical Geology,
248 v. 266, p. 157–170, doi:10.1016/j.chemgeo.2009.06.001.

Giovanni, M.K., 2007, Tectonic and Thermal Evolution of the Cordillera Blanca Detachment System, Peruvian Andes: Implication for Normal Faulting in a Contractionnal Orogen [Thesis (unpublished)]: Los Angeles, University of California–Los Angeles, p. 1–255.

Giovanni, M.K., Horton, B.K., Garzione, C.N., McNulty, B., and Grove, M., 2010, Extensional basin evolution in the Cordillera Blanca, Peru: Stratigraphic and isotopic records of detachment faulting and orogenic collapse in the Andean hinterland: Tectonics, v. 29, TC6007, doi:10.1029/2010TC002666.

Gutscher, M.A., Olivet, J.L., Aslanian, D., Eissen, J.P., and Maury, R., 1999, The "lost Inca Plateau": cause of flat subduction beneath Peru?: Earth and Planetary Science Letters, v. 171, p. 335–341, doi:10.1016/S0012-821X(99)00153-3.

Hodson, K.R., 2012, Morphology, exhumation, and Holocene erosion rates from a tropical glaciated mountain range: The Cordillera Blanca, Peru [Thesis (unpublished)]: Montréal, McGill University, p. 1–94.

Hoorn, C., et al., 2010, Amazonia Through Time: Andean Uplift, Climate Change, Landscape Evolution, and Biodiversity: Science, v. 330, no. 6006, p. 927–931, doi:10.1126/science.1194585.

von Huene, R., and Suess, E., 1988, Ocean Drilling Program Leg 112, Peru continental margin: Part 1, Tectonic History: Geology, v. 16, p. 934–938, doi: 10.1130/0091-7613(1988)016<0934:ODPLPC>2.3.CO;2.

INGEMMET (El Instituto Geológico Minero y Metalúrgic), 1999, Mapa geológico del Perú: Peru, Instituto Geológico, Minero y Metalúrgico, Sector Energía y Minas, 1:1,000,000.

Ketcham, R.A., Carter, A., Donelick, R.A., Barbarand, J., and Hurford, A.J., 2007, Improved measurement of fission-track annealing in apatite using c-axis projection: The American Mineralogist, v. 92, p. 789–798, doi:10.2138/am.2007.2280.

McLaughlin, D.H., 1924, Geology and physiography of the Peruvian Cordillera, departments of Junin and Lima: Geological Society of America Bulletin, v. 35, p. 591–632, doi:10.1130/GSAB-35-591.

McNulty, B.A., and Farber, D.L., 2002, Active detachment faulting above the Peruvian flat slab: Geology, v. 30, p. 567–570, doi:10.1130/0091-7613(2002)030<0567:ADFATP>2.0.CO;2.

McNulty, B.A., Farber, D.L., Wallace, G.S., Lopez, R., and Palacios, O., 1998, Role of plate kinematics and plate-slip-vector partitioning in continental magmatic arcs: Evidence from the Cordillera Blanca, Peru: Geology, v. 26, p. 827–830, doi:10.1130/0091-7613(1998)026<0827:ROPKAP>2.3.CO;2.

Mégard, F., 1987, Structure and evolution of the Peruvian Andes: The anatomy of mountain ranges, *in* Schaer, J.P., and Rodgers J., eds., The Anatomy of Mountain Ranges: Princeton, New Jersey, Princeton University Press, p. 179–210.

Michalak, M.J., 2013, Exhumation of the Peruvian Andes: Insights from Mineral Chronometers [Ph.D. thesis]: Santa Cruz, California, University of California, p. 1–166.

Montario, M.J., 2001, Exhumation of the Cordillera Blanca, Northern Peru, based on apatite fission track analysis [Thesis (unpublished)]: Schenectady, New York, Union College, Department of Geology, p. 1–12.

294 Mukasa, S.B., 1984, Comparative Pb isotope systematics and zircon U-Pb geochronology
295 for the Coastal San Nicolas and Cordillera Blanca batholiths, Peru [Thesis
296 (unpublished)]: Santa Barbara, University of California–Santa Barbara, p. 1-362.
297 Myers, J.S., 1976, Erosion surfaces and ignimbrite eruption, measures of Andean uplift in
298 northern Peru: Geological Journal, v. 11, p. 29–44, doi:10.1002/gj.3350110104.
299 Noble, D.C., McKee, E.H., Mourier, T., and Mégard, F., 1990, Cenozoic stratigraphy,
300 magmatic activity, compressive deformation, and uplift in northern Peru: Geological
301 Society of America Bulletin, v. 102, p. 1105–1113, doi:10.1130/0016-
302 7606(1990)102<1105:CSMACD>2.3.CO;2.
303 Petford, N., and Atherton, M.P., 1992, Granitoid emplacement and deformation along a
304 major crustal lineament: the Cordillera Blanca, Peru: Tectonophysics, v. 205, p. 171–
305 185, doi:10.1016/0040-1951(92)90425-6.
306 Ramos, V.A., and Folguera, A., 2009, Andean flat-slab subduction through time:
307 Geological Society of London, Special Publications, v. 327, p. 31–54,
308 doi:10.1144/SP327.3.
309 Rosenbaum, G., Giles, D., Saxon, M., Betts, P.G., Weinberg, R.F., and Duboz, C., 2005,
310 Subduction of the Nazca Ridge and the Inca Plateau: Insights into the formation of
311 ore deposits in Peru: Earth and Planetary Science Letters, v. 239, p. 18–32,
312 doi:10.1016/j.epsl.2005.08.003.
313 Wipf, M., 2006, Evolution of the Western Cordillera and Coastal Margin of Peru:
314 Evidence from low-temperature Thermochronology and Geomorphology: Zürich,
315 Swiss Federal Institute of Technology, p. 1–163.

316 Wise, J.M., and Noble, D.C., 2003, Geomorphic evolution of the Cordillera Blanca,
317 Northern Peru: Boletín de la Sociedad Geológica del Perú, v. 96, p. 1–21.

318 **FIGURE CAPTIONS**

319 Figure 1. A) Study area location within the Peruvian flat-slab and the South America
320 Pacific margin (modified after Ramos and Folguera, 2009). The respective positions of
321 the Nazca Ridge (NR) at ~15 Ma, 0 Ma; and of the Inca plateau (IP) at ~13 Ma
322 (Rosenbaum et al., 2005) are represented in red. B) Geological map of the Cordillera
323 Occidental (northern Peru) showing AFT ages (red) and AHe ages (blue) (modified from
324 INGEMMET geologic map of Ancash; INGEMMET, 1999.
325
326 Figure 2. Age-elevation plots and Temperature-time (Tt) paths predicted for
327 thermochronological ages using Gautheron et al. (2009) He diffusion model. A-C) Age-
328 elevation plots showing AFT ages (red), mean track length (MTL; yellow) and AHe ages
329 (blue), ages predicted by the thermal history are plotted in pastel colors. Northern
330 Cordillera Negra (CN) profile (A), southern CN profile (B), and Cordillera Blanca (CB)
331 profile (C). D-F) Tt paths for northern/southern CN, and CB profiles. Each line represents
332 the Tt path of a sample; red line represents the path of the lowest elevation sample and
333 blue line the highest, pastel shading represent uncertainties.
334
335 Figure 3. Block diagrams showing the uplift history and paleogeography of the Cordillera
336 Occidental in northern Peru. Diagrams represent surface uplift (bold arrow), volcanism
337 (black triangle), partial melting (red droplet), faults (dotted and continuous black lines),
338 drainage network, and the CB batholith. A) The Calipuy Formation emplaces in the CN

above a “normal” subduction (54–15 Ma). B) Subduction of the NR, slab flattening, and corresponding surface uplift in the CN at 15 Ma. C) During the slab flattening, magmatism shutdowns in the CN and moves eastward. The CB batholith emplaces at depth and is exhumed in a strike-slip context. D) The CBNF accommodates the recent exhumation of the CB resulting in modern elevations >6 km.

[1]GSA Data Repository item 2015xxx, xxxxxxxx, is available online at www.geosociety.org/pubs/ft2015.htm, or on request from editing@geosociety.org or Documents Secretary, GSA, P.O. Box 9140, Boulder, CO 80301, USA.

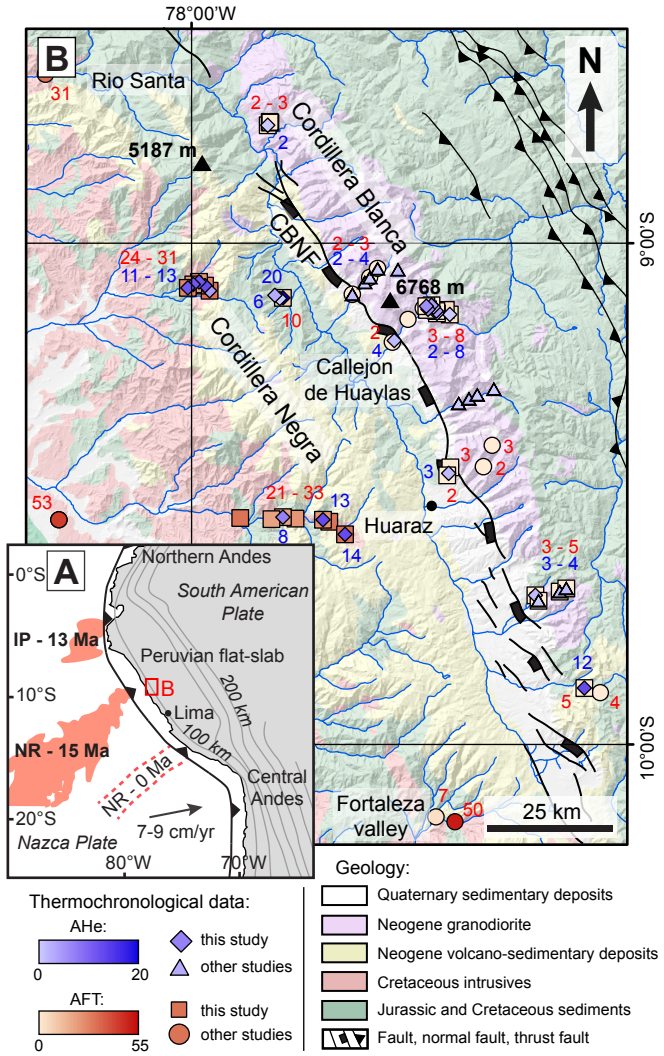
78°00'W
9°00'S
10°00'S
B
Rio Santa
N
5187 m
Cordillera Blanca
CBNF
6768 m
Cordillera Negra
Callejon
de Huaylas
Huaraz
Fortaleza
valley
25 km
A
0°S
10°S
20°S
80°W
70°W
Northern Andes
South American
Plate
IP - 13 Ma
Peruvian flat-slab
B
Lima
200 km
100 km
NR - 15 Ma
NR - 0 Ma
Central
Andes
7-9 cm/yr
Nazca Plate
Thermochronological data:
AHe:
0
20
this study
other studies
AFT:
0
55
this study
other studies
Geology:
Quaternary sedimentary deposits
Neogene granodiorite
Neogene volcano-sedimentary deposits
Cretaceous intrusives
Jurassic and Cretaceous sediments
Fault, normal fault, thrust fault

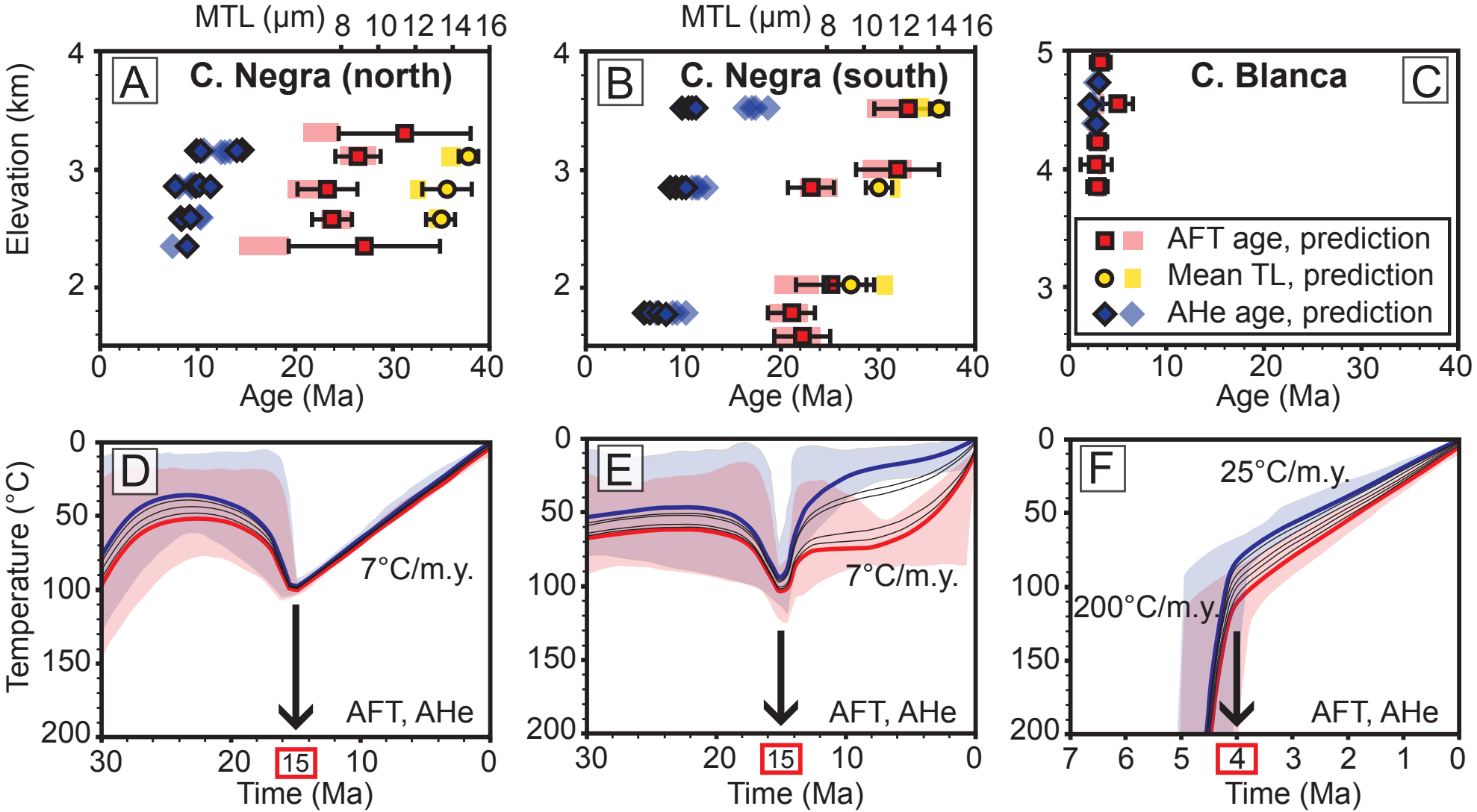
MTL (μm) 8 10 12 14 16
A
C. Negra (north)
Elevation (km)
4
3
2
0 10 20 30 40
Age (Ma)
MTL (μm) 8 10 12 14 16
B
C. Negra (south)
4
3
2
0 10 20 30 40
Age (Ma)
C
C. Blanca
5
4
3
AFT age, prediction
Mean TL, prediction
AHe age, prediction
0 10 20 30 40
Age (Ma)
D
Temperature (°C)
0
50
100
150
200
7°C/m.y.
AFT, AHe
30 20 15 10 0
Time (Ma)
E
0
50
100
150
200
7°C/m.y.
AFT, AHe
30 20 15 10 0
Time (Ma)
F
0
50
100
150
200
25°C/m.y.
200°C/m.y.
AFT, AHe
7 6 5 4 3 2 1 0
Time (Ma)

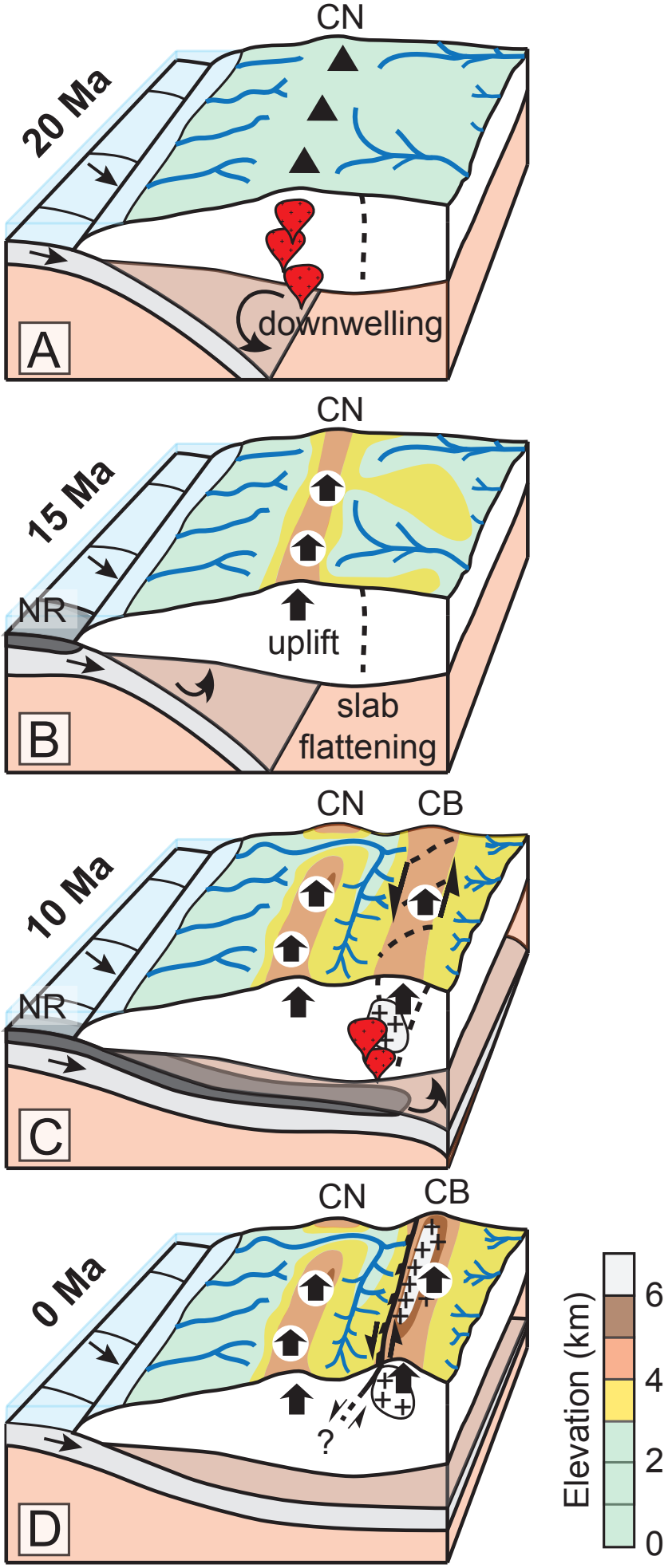
CN
20 Ma
downwelling
A
CN
15 Ma
NR
uplift
slab
flattening
B
CN
CB
10 Ma
NR
C
CN
CB
0 Ma
?
D
Elevation (km)
6
4
2
0